JOURNAL OF AGRICULTURAL AND FOOD CHEMISTRY

pubs.acs.org/JAFC

Article

Fluorescence Resonance Energy Transfer Aptasensor of Ochratoxin A Constructed Based on Gold Nanorods and DNA Tetrahedrons

Liling Hao, Mengqiu Li, Kaimin Peng, Tai Ye, Xiuxiu Wu, Min Yuan, Hui Cao, Fengqin Yin, Huajie Gu, and Fei Xu*

Cite This: *J. Agric. Food Chem.* 2022, 70, 10662−10668

Read Online

ACCESS | Metrics & More | Article Recommendations | Supporting Information

ABSTRACT: Ochratoxin A (OTA) contamination of corn has received significant attention due to the wide distribution and high toxicity of OTA. The maximum residue limit standard of OTA in corn has been established by the Chinese Government and other unions. Nanoparticle-based fluorescence resonance energy transfer (FRET) assays are promising methods for the sensitive and fast detection of OTA. However, satisfactory detection sensitivity is commonly achieved with complicated signal amplification processes or specific nanoparticle morphologies, which means that these assays are not conducive to fast detection. This study proposes a simple and novel strategy to improve the sensitivity of FRET aptasensors. In this strategy, a DNA tetrahedron was first used in gold nanorod-based FRET aptasensors. DNA tetrahedron-modified gold nanorods are used as fluorescent acceptors, and Cy5-modified complementary sequences of the OTA aptamer are used as fluorescent donors. The aptamers of OTA are embedded in the DNA tetrahedrons, and FRET occurs when the aptamers hybridize with the Cy5-modified complementary sequences. The aptamer-integrated DNA tetrahedron modified on the surface of gold nanorods acts as an anchor, thus avoiding the crowding and entanglement of aptamers. Due to the competitive combination between the OTA aptamers and complementary sequences, the greater the amount of OTA, the less the amount of Cy5-modified complementary sequences that bind with the aptamers and the less the amount of Cy5 that is quenched. Thus, the fluorescence intensity is positively related to the OTA concentration. In this study, in the concentration range of 0.01−10 ng/mL, the fluorescence intensity was found to be linearly related to the logarithmic concentration of OTA. The limit of detection was calculated to be 0.005 ng/mL. The specificity of the developed biosensor was demonstrated to be efficient. The accuracy and stability of the developed aptasensor were also tested, and the method exhibited good performance in real samples.

KEYWORDS: *fluorescence resonance energy transfer, DNA tetrahedron, aptamer*

INTRODUCTION

Ochratoxin A (OTA) is one of the most common mycotoxins found in agricultural products, especially grains.[1] It is a secondary metabolite produced by poisonous fungi species such as *Aspergillus* and *Penicillium* under appropriate temperature and humidity conditions.[2,3] Research has confirmed that OTA exposure can lead to nephrotoxicity, hepatotoxicity, immune system toxicity, and carcinogenicity; OTA is classified as a class 2B toxin by the International Agency for Research on Cancer (IARC).[4] Corn is often polluted by OTA during harvest and storage, and due to its stability, OTA is difficult to destroy during subsequent food processing. As such, corn has one of the highest detection frequencies of OTA among all food materials.[5] A maximum residue limit of OTA in corn has been set at 5 ng/g by the Chinese Government and other international organizations, such as the European Union.[6] Therefore, it is critical to develop a sensitive detection method for OTA to monitor its concentration in food materials.

Detection methods based on chromatography and mass spectrometry techniques have been used for OTA detection.[7,8] These methods are commonly used due to their high sensitivity and accuracy. However, chromatography technique-based instruments are sophisticated and expensive and rarely meet the need for fast, real-time monitoring of OTA. Biosensors based on nanotechnologies and antibodies or aptamers as recognition elements are good alternatives for the rapid detection of OTA in corn.[9−14] Among these, fluorescence resonance energy transfer (FRET)-based biosensors have several advantages, including the availability of fluorescent molecules, high luminescence efficiency, fast response, and high sensitivity.[15] Further, the simple assay technique avoids complicated separation during detection, making it more suitable for fast detection. However, due to the complex food matrix, the sensitivity of FRET-based OTA detection methods still requires improvement.

The current approaches to obtaining satisfactory detection sensitivity with nanoparticle-based FRET assays mainly involve complicated signal amplification processes or specific morphologies of nanoparticles. The commonly used signal amplification methods are rolling circle amplification,[16,17] hybridization chain reaction,[18] and target-catalyzed hairpin

Received: May 24, 2022
Revised: July 26, 2022
Accepted: July 27, 2022
Published: August 8, 2022

assembly technology,[19] which require the design of complicated DNA sequences or expensive enzymes. Nanoparticles with specific morphologies, such as upconversion nanoparticles,[20,21] metal−organic frameworks[22] and core−shell nanoparticles,[23−25] are often sophisticated and hard to prepare. Thus, they are not conducive to the establishment of rapid detection methods.

Improving the performance of recognition elements is another promising approach to obtaining satisfactory detection sensitivity. Aptamers are single-stranded DNA or RNA oligonucleotide sequences that can combine with their target specifically. Compared with antibodies, aptamers possess better chemical stability and less interbatch differences and are easier to modify, which makes aptamers more widely used. An increasing number of studies have focused on nanoparticle-based aptasensors for the fast detection of OTA. However, crowding and entanglement of the aptamers that assemble on the surface of the nanoparticles disrupt recognition and binding between the aptamers and their target,[26] thus affecting detection sensitivity.

The DNA tetrahedron is composed of four DNA strands in the shape of a tetrahedron. The specific DNA nanostructure possesses significant advantages, such as easy operation, structural stability, and well-controlled density and orientation.[27] Therefore, DNA tetrahedrons can be used in aptamer-based biosensors to avoid the crowding and entanglement of aptamers on the surface of electrodes[28] or other nanoparticles; this may improve the strand hybridization efficiency and detection sensitivity.[29]

Herein, a simple and convenient strategy to improve the sensitivity of FRET aptasensors is proposed. This strategy involves the use of a DNA tetrahedron in gold nanorod-based FRET aptasensors. Specifically, DNA tetrahedron-modified gold nanorods are used as fluorescent acceptors, and Cy5-modified complementary sequences of OTA aptamers are used as fluorescent donors. The aptamers of OTA are embedded in the DNA tetrahedron, and FRET occurs when the aptamers hybridize with the Cy5-modified complementary sequences. The aptamer-integrated DNA tetrahedron modified on the surface of the gold nanorods acts as an anchor to avoid the crowding and entanglement of aptamers. Thus, due to the competitive combination between the aptamers with OTA and the complementary sequences, the concentration of OTA can be sensitively detected by determining the fluorescence intensity of the detection system.

MATERIALS AND METHODS

Materials and Instruments. OTA, zearalenone (ZEN), T-2 toxin (T-2), aflatoxin B1 (AFB1), and ochratoxin B (OTB) were provided by QingDao Pribolab Biological Engineering Co., Ltd. (Qingdao, China). Chlorauric acid ($HAuCl_4$), citrate sodium, sodium borohydride ($NaBH_4$), and silver nitrate ($AgNO_3$) were purchased from Sinopharm Chemical Reagent Co., Ltd. (Shanghai, China). SH-PEG was purchased from Sigma-Aldrich (Shanghai) Trading Co., Ltd. Hexadecyl trimethyl ammonium bromide (CTAB) was purchased from Beijing Innochem Science and Technology Co., Ltd, (Beijing, China). Tris(2-carboxyethyl) phosphine hydrochloride (TCEP) (purity >98.0%) and L-ascorbic acid were bought from TCI Development Co., Ltd. (Shanghai, China). The corn sample was purchased from a local supermarket. The oligonucleotides were synthesized by Shanghai Generay Biotech Co., Ltd. (Shanghai, China) and are shown in Table S1.

Apparatus. A JEOL model 2100HR instrument was used for transmission electron microscopy (TEM) (JEOL Ltd., Japan). The fluorescence intensity was measured by a Biotek Synergy H1 (Agilent Technologies, Inc. USA). The electrophoresis experiment was performed with a vertical electrophoresis apparatus (BIO-RAD, USA), and the gel was detected by a ChemiDoc XRS+ imager (Bio-RAD, USA). A UV-1800 spectrophotometer was used to record the ultraviolet−visible (UV−vis) absorption spectra (Shimadzu, Japan).

Preparation and Characterization of Gold Nanorods (AuNRs). AuNRs were synthesized according to Guo's method[30] via seed-mediated growth routes. Gold seeds were first prepared by adding 0.122 mL of 23.7 mM $HAuCl_4$ to 7.5 mL of 0.05 M CTAB solution. After mixing, 0.6 mL of ice-cooled 0.01 M $NaBH_4$ was rapidly added to the above solution and mixed. The mixture was incubated at 40°C in a water bath for 2 h to obtain CTAB-protected gold seeds. Then, 0.055 mL of 0.01 M $AgNO_3$ was added to 30 mL of 0.05 M CTAB under stirring; 0.735 mL of 23.7 mM $HAuCl_4$ was then added, and the solution changed to dark yellow. Subsequently, 0.24 mL of 0.1 M ascorbic acid was added to the above solution under vigorous stirring until the solution turned colorless. Finally, the growth solution was obtained by adding 0.3 mL of the freshly prepared gold seeds. The growth solution was then incubated for 3 h. The prepared AuNRs were then centrifuged to remove the excess surfactant and redispersed in water for further use. The morphology and particle size of the prepared AuNRs were characterized by TEM. The UV−vis absorption spectrum of the AuNRs was measured by a UV-1800 spectrophotometer.

Preparation and Characterization of DNA Tetrahedrons. Four strands (tetra A, tetra B, tetra C, and tetra D) were dissolved in TE buffer (10 mM Tris, 1.0 mM EDTA, pH 8.0) with a final concentration of 50 μM. First, 2.5 μL of each of the above four strands was added to 30 μL of TM buffer (20 mM Tris, 50 mM $MgCl_2$, pH 8.0), and 10 μL of TCEP was then added to the above solution at 37°C for 12 h to activate the thiolated DNA. The above mixture was then heated at 95°C for 10 min and cooled to 4°C for 5 min to form a three-dimensional DNA tetrahedron. The prepared DNA tetrahedron was verified by native polyacrylamide gel electrophoresis (PAGE).

Preparation and Characterization of AuNRs−DNA Tetrahedron. The conjugation of AuNRs and the DNA tetrahedron was performed as follows. First, 100 μL of the redispersed AuNRs, 10 μL of DNA tetrahedron, and 10 μL of 5×10^{-5} M SH-PEG were incubated at 37°C for 2 h. Then, the mixture was centrifuged at 10000 rpm for 10 min to remove the unbound DNA tetrahedron, and the precipitate was redispersed to obtain the conjugation of AuNRs and the DNA tetrahedron. UV−vis absorption spectroscopy and native PAGE were used to characterize the conjugation of AuNRs and the DNA tetrahedron.

Detection of OTA. First, series concentrations of OTA and 4 μL of 10 μM complementary sequences were incubated with 100 μL of AuNRs−DNA tetrahedron at 37°C. Then, the fluorescence intensity of the mixture was detected by a Biotech H1 microplate reader at an excitation wavelength of 674 nm. All measurements were performed in triplicate.

Application in the Corn Sample. The corn sample was ground and dried at 50°C. The corn powder was then mixed with three gradient concentrations of OTA and incubated at 25°C for 2 h. Briefly, 25 mL of methanol/water (7:3, v/v) was added to 5.0 g of the prepared sample. Then, the mixture was incubated at 25°C for 10 min. Next, the mixture was centrifuged at 5000 rpm/min for 10 min, and the supernatant was filtered through a 0.22 μm membrane. The filtrate was diluted with binding buffer (10 mmol/L Tris, 120 mmol/L NaCl, 5 mmol/L KCl, and 20 mmol/L $CaCl_2$, pH 8.5). Standard addition and recovery experiments and relative standard deviation (RSD) detection were performed as described in the Detection of OTA section.

RESULTS AND DISCUSSION

Principle of the FRET Aptasensor. The typical FRET system for the detection of OTA based on Cy5 and AuNRs is

https://doi.org/10.1021/acs.jafc.2c03626
J. Agric. Food Chem. 2022, 70, 10662−10668

Scheme 1. Principle of the FRET Aptasensor for the Detection of OTA Based on AuNRs and DNA Tetrahedrons

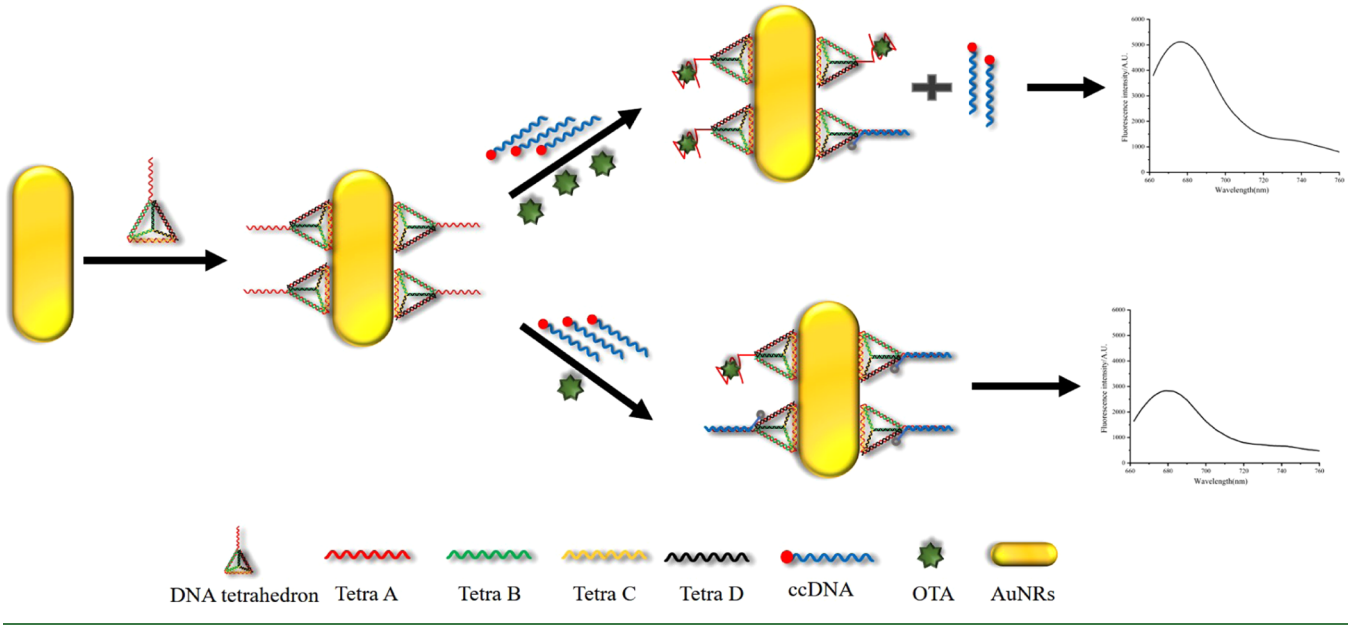

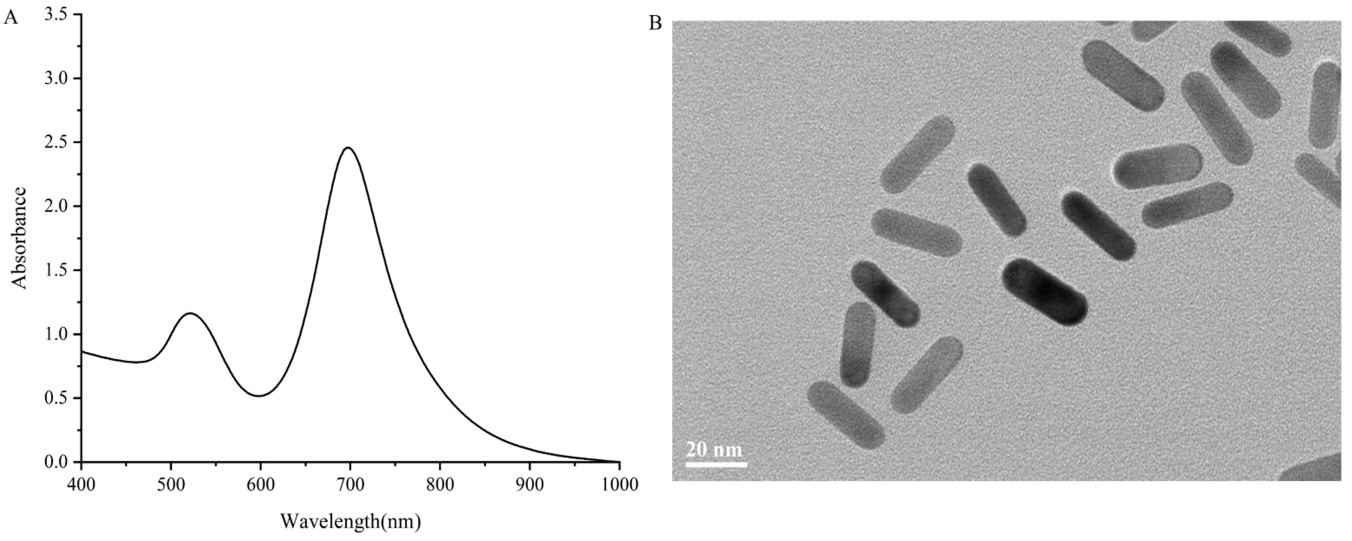

Figure 1. UV−vis spectra (A) and TEM image (B) of the prepared AuNRs.

illustrated in Scheme 1. Four DNA strands including an OTA aptamer sequence were first assembled to form a DNA tetrahedron; this DNA tetrahedron can specifically combine with OTA by integrating the OTA aptamer with the DNA strands. Then, the thiolated DNA tetrahedron was fixed on the surface of AuNR through an Au-S bond to form the acceptor probe. A Cy5-labeled complementary sequence was used as the donor probe; this can combine with the acceptor probe through DNA base pairing. FRET occurs when the Cy5 and AuNR are brought into close proximity and when the emission spectrum of the donor and the absorbance spectrum of the acceptor overlap well. In the presence of OTA, the Cy5-labeled complementary sequence and OTA can competitively combine with the capture probe. The greater the concentration of OTA, the less Cy5-labeled complementary sequences that combine with the acceptor probes, and the higher the fluorescence intensity of the system. Thus, the concentration of OTA can be detected by measuring the fluorescence intensity of the system, which is positively correlated with the OTA concentration.

Characterization of AuNRs and the DNA Tetrahedron. The UV−vis spectrum (Figure 1A) showed that the AuNRs exhibited two typical surface plasma resonance (SPR) modes, resulting in two resonance absorption bands at approximately 521 and 699 nm. The TEM image of the AuNRs shows that the prepared AuNRs were approximately 12 nm in width and 30 nm in length; the aspect ratio was approximately 2.5 (Figure 1B).

Successful preparation of the DNA tetrahedron was critical for this assay. Thus, the DNA tetrahedron was characterized by native PAGE. The results are shown in Figure 2A, with the addition of tetra C (lane 4), tetra C and tetra D (lane 3), tetra C, tetra D, and tetra A (lane 2) to tetra B, the electrophoretic mobility of the complexes showed a decreasing trend. This may be because the addition of DNA increases the molecular mass of the DNA complexes. Thus, the results indicate that the DNA tetrahedron was successfully prepared.

Characterization of the Conjugation of AuNRs−DNA Tetrahedron. The acceptor probe in this assay was prepared

https://doi.org/10.1021/acs.jafc.2c03626
J. Agric. Food Chem. 2022, 70, 10662−10668

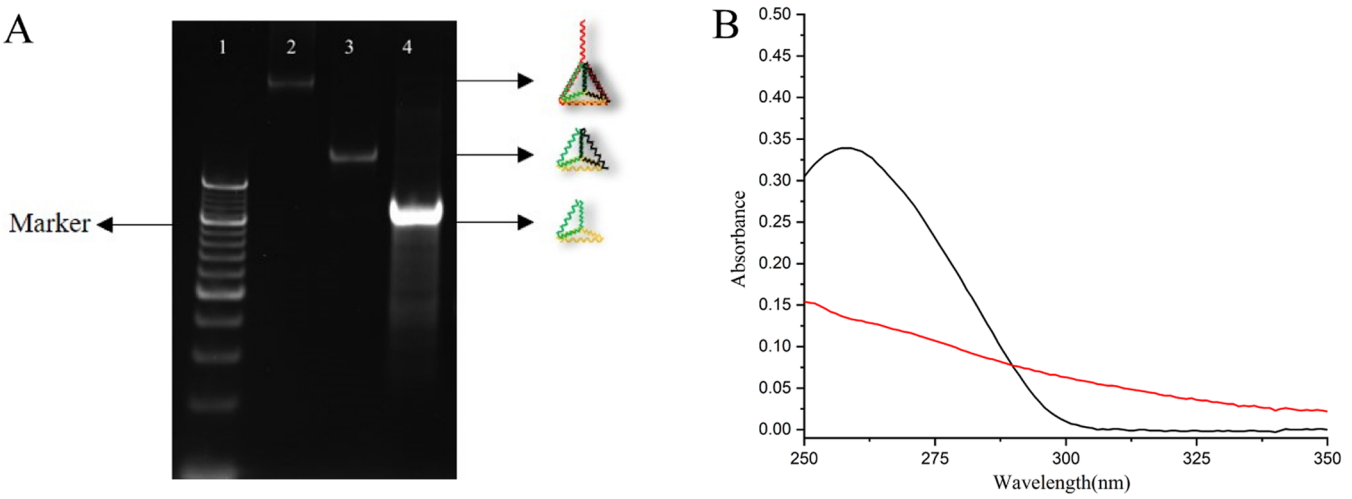

Figure 2. (A) Results of the native PAGE experiment for verification of the DNA tetrahedron, lane 1: DNA marker, lane 2: the prepared DNA tetrahedron, lane 3: tetra D + tetra C + tetra B, lane 4: tetra C + tetra B; B: UV−vis spectra of the DNA tetrahedron (black line) and supernatant liquor after conjugation of the DNA tetrahedron with the AuNRs (red line).

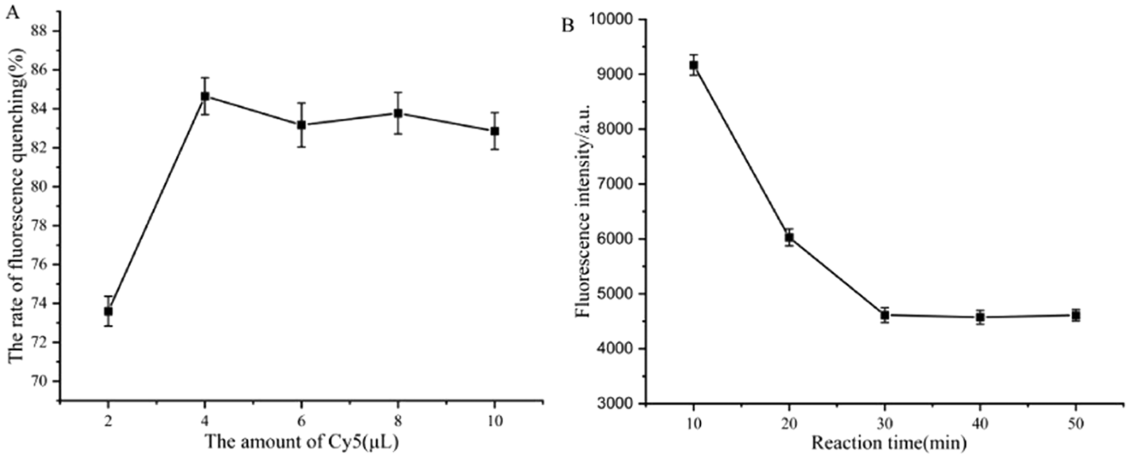

Figure 3. (A) Effect of the amount of Cy5-modified complementary sequences (2, 4, 6, 8, 10 μL) on the rate of fluorescence quenching. (B) Effect of the FRET reaction time (10, 20, 30, 40, 50 min) on the fluorescence intensity.

by the conjugation of AuNRs with the SH-DNA tetrahedron. The prepared AuNRs were positively charged with the addition of CTAB, causing nonspecific adsorption of DNA sequences. Thus, SH-PEG was used to avoid nonspecific adsorption, and the UV−vis absorption change of the supernatant before and after the conjugation of AuNRs with the SH-DNA tetrahedron was used to verify the successful assembly of the acceptor probe. As shown in Figure 2B, there was a significant reduction in the absorption at 260 nm resulting from the reduced DNA tetrahedron in the supernatant, indicating the successful binding of the SH-DNA tetrahedron with AuNRs. PAGE was also used to further characterize the conjugation. As shown in Figure S1, a bright band was observed after conjugation of the DNA tetrahedron with the AuNRs (lane 2 and lane 3), indicating successful preparation of the acceptor probe.

Optimization of the Experimental Conditions. The amount of Cy5-modified complementary sequences plays an important role in the competition detection; thus, this amount was optimized. The results in Figure 3A indicate that, with an increase in the amount of Cy5-modified complementary sequences, the rate of fluorescence quenching of the system first increased and then reached a plateau. This is possibly because the combination of the DNA tetrahedron with the Cy5-modified complementary sequences reached saturation at 4.0 μL. Therefore, the optimal amount of Cy5-modified complementary sequences is 4.0 μL.

The effect of the FRET reaction time on the fluorescence intensity with an OTA concentration of 1 ng/mL was also studied. As shown in Figure 3B, with an increase in the reaction time, the fluorescence intensity first decreased and then reached a plateau. This may be because the FRET reaction needs 30 min to achieve equilibrium. Thus, 30 min was selected as the optimal FRET reaction time.

Analytical Performance. The UV−vis absorption spectrum of AuNRs and the fluorescence spectrum of Cy5 were measured. The results revealed that AuNRs exhibited broad absorption that largely overlapped with the fluorescence spectrum (Figure 4). This indicates that Cy5 and the prepared AuNRs act as a suitable FRET donor/acceptor pair.

In the presence of OTA, OTA and Cy5-modified complementary sequences competitively bind to the aptamers that are integrated with the DNA tetrahedron. The Cy5-modified complementary sequences that bind with the

https://doi.org/10.1021/acs.jafc.2c03626
J. Agric. Food Chem. 2022, 70, 10662−10668

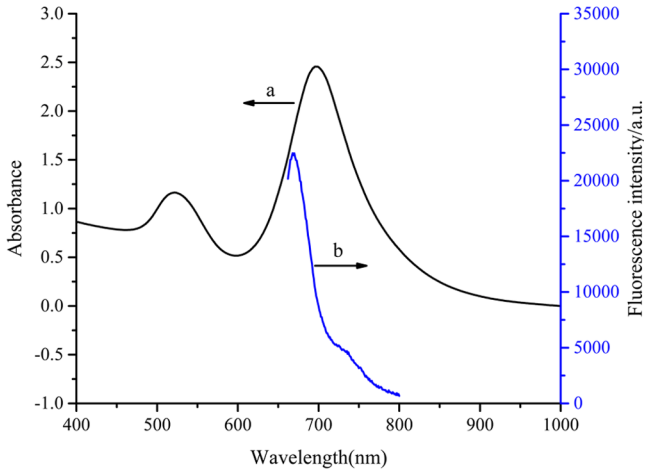

Figure 4. UV−vis spectra of AuNRs (a) and fluorescence spectrum of Cy5 (b).

aptamers and are assembled on the surface of AuNRs will be quenched by AuNRs. The greater the amount of OTA, the less Cy5-modified complementary sequences that bind with the aptamers and the less Cy5 that is quenched. Thus, the fluorescence intensity is positively related to the OTA concentration.

As shown in Figure 5A,B, with increasing concentrations of OTA, the fluorescence intensity at 674 nm increased. Under optimal conditions, ΔFL (ΔFL = FL − FL0, where FL and FL0 refers to the fluorescence intensity with OTA and the background fluorescence intensity, respectively) was positively related to the logarithm of the concentration of OTA. With an OTA concentration between 0.01−10 ng/mL, ΔFL was linearly correlated with the logarithm of the concentration of OTA with the following equation: $Y = 1786.3 + 517.46 \times X$ ($R^2 = 0.9922$). The detection limit of OTA was obtained through the equation LOD = 3SD/m (SD is the standard deviation of the blank and m is the slope of the calibration plot), and its value was 0.005 ng/mL. Some other reported detection methods for OTA have been listed in Table S1. The developed method shows a comparable linear range and lower limit of detection, which may be attributed to the use of DNA tetrahedron-integrated aptamers with AuNR-based FRET detection mode.

Specific detection of OTA is critical for the aptasensor. Structural analogues of OTA and toxins that possibly coexist with OTA, including ochratoxin B (OTB), zearalenone (ZEN), aflatoxin B1 (AFB1), and T-2 toxin (T-2), were used to test the specificity of the aptasensor. The relative fluorescence intensity ratio was calculated by adding 1 ng/mL of OTA and other toxins to the FRET system and determining the fluorescence intensity according to the above procedures. The relative fluorescence intensity ratio was determined by the formula (FL − FL0)/(FLA − FL0), where FL0, FL, and FLA represent the fluorescence intensity of the blank sample, the fluorescence intensity of the other toxins, and the fluorescence intensity of OTA, respectively. The results are presented in Figure 5C. The lower relative fluorescence intensity ratio values of the other toxins indicate that the aptasensor has high specificity.

Artificially contaminated corn was then selected as a real sample to test the suitability of the developed aptasensor. The corns were spiked with concentrations of 1, 2, and 10 ng/mL OTA, and the recovery rates were determined by both the developed aptasensor and a commercial ELISA kit. Table 1 shows that the results determined from the developed aptasensor were consistent with those from the ELISA kit; the mean recovery rates of the FRET assay and ELISA were 92.6−104.7 and 93.8−106.1%, respectively. The above results show that the developed FRET assay has good accuracy and can be applied to real samples.

In conclusion, in this study, a novel and convenient FRET assay was developed to improve the sensitivity of FRET aptasensors. A DNA tetrahedron was introduced to the detection system to avoid the crowding and entanglement of DNA on the surface of nanoparticles, thus improving the detection sensitivity of the assay. In this work, the DNA tetrahedron that was integrated with the OTA aptamer was modified on the surface of gold nanorods and served as the acceptor; Cy5-modified complementary sequences served as the donor. Thus, FRET accrues in the case of the complementary base binding between the aptamer and the Cy5-modified complementary sequences. OTA will bind with the aptamer and thus influence the FRET, leading to changes in the fluorescence intensity. The results of this study revealed that, under optimal experimental conditions, the FRET assay exhibited highly sensitive performance with an OTA detection limit of 0.005 ng/mL. In addition, we evaluated the accuracy and availability in real corn samples, and the results obtained by the developed aptasensor displayed satisfactory consistency with the commercial detection methods. The results

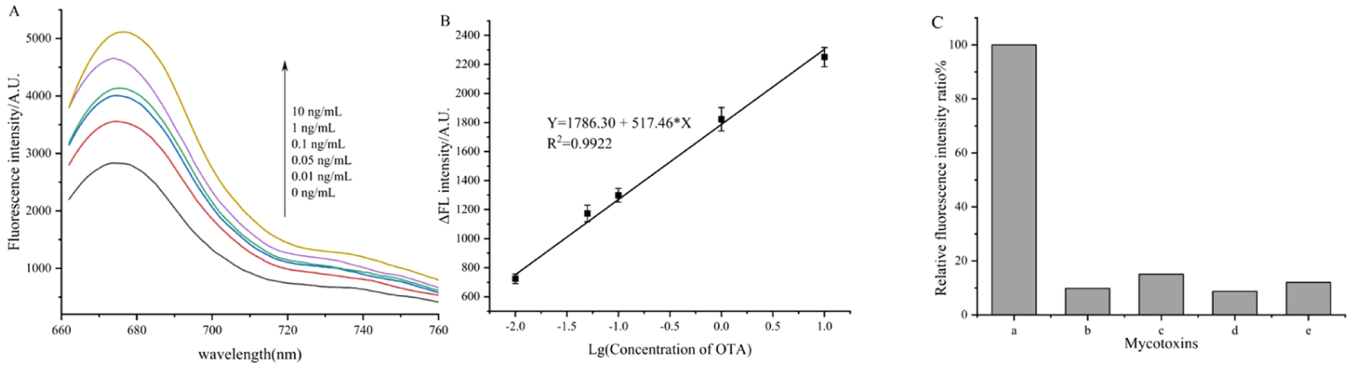

Figure 5. Fluorescence spectra of the system with different OTA concentrations (A); linear relationship between the fluorescence intensity at 674 nm measured by the aptasensor and the logarithm of the OTA concentration (B); specificity verification of the detection method for OTA with other mycotoxins, a: OTA, b: AFB_1, c: OTB, d: T-2 and e: ZEN (C).

https://doi.org/10.1021/acs.jafc.2c03626
J. Agric. Food Chem. 2022, 70, 10662−10668

Table 1. Detection Results of OTA Concentrations in Corn with the Developed Aptasensor and ELISA Kit

items	added concentration (ng/mL)	results determined by ELISA (ng/mL)	recovery rate calculated by ELISA (%)	results obtained by this method (ng/mL)	recovery calculated by this method (%)	RSD of this method (%)
corn	0	ND[a]		ND[a]		
corn	1	1.027 ± 0.04	102.7	0.926 ± 0.05	92.6	5.40
corn	1	1.061 ± 0.05	106.1	0.937 ± 0.06	93.7	6.40
corn	2	1.908 ± 0.07	95.4	2.094 ± 0.14	104.7	6.69
corn	2	1.946 ± 0.09	97.3	1.972 ± 0.09	98.6	4.56
corn	10	9.384 ± 0.36	93.8	9.642 ± 0.47	96.4	4.87
corn	10	9.853 ± 0.33	98.5	9.473 ± 0.39	94.7	4.12

[a]ND: not detected.

demonstrated that the developed assay has good accuracy and can be successfully applied to real samples. However, in this work, the fluorescence intensity was determined by a fluorescence microplate reader, which may limit its application for onsite detection. It remains a challenge and a goal to further develop a portable detector for onsite food safety detection, such as smartphones, and so on, in the future.

■ ASSOCIATED CONTENT

Supporting Information

The Supporting Information is available free of charge at https://pubs.acs.org/doi/10.1021/acs.jafc.2c03626.

Results of the PAGE experiment for verification of the conjugation between the DNA tetrahedron and AuNRs (Figure S1); DNA sequences used in this work (Table S1); the current detection methods for OTA (Table S2) (PDF)

■ AUTHOR INFORMATION

Corresponding Author

Fei Xu − *School of Health Science and Engineering, Shanghai Engineering Research Center for Food Rapid Detection, University of Shanghai for Science and Technology, Shanghai 200093, China;* orcid.org/0000-0001-7745-2855; Email: xufei8135@126.com

Authors

Liling Hao − *School of Health Science and Engineering, Shanghai Engineering Research Center for Food Rapid Detection, University of Shanghai for Science and Technology, Shanghai 200093, China*

Mengqiu Li − *School of Health Science and Engineering, Shanghai Engineering Research Center for Food Rapid Detection, University of Shanghai for Science and Technology, Shanghai 200093, China*

Kaimin Peng − *School of Health Science and Engineering, Shanghai Engineering Research Center for Food Rapid Detection, University of Shanghai for Science and Technology, Shanghai 200093, China*

Tai Ye − *School of Health Science and Engineering, Shanghai Engineering Research Center for Food Rapid Detection, University of Shanghai for Science and Technology, Shanghai 200093, China;* orcid.org/0000-0002-7789-6920

Xiuxiu Wu − *School of Health Science and Engineering, Shanghai Engineering Research Center for Food Rapid Detection, University of Shanghai for Science and Technology, Shanghai 200093, China*

Min Yuan − *School of Health Science and Engineering, Shanghai Engineering Research Center for Food Rapid Detection, University of Shanghai for Science and Technology, Shanghai 200093, China*

Hui Cao − *School of Health Science and Engineering, Shanghai Engineering Research Center for Food Rapid Detection, University of Shanghai for Science and Technology, Shanghai 200093, China*

Fengqin Yin − *School of Health Science and Engineering, Shanghai Engineering Research Center for Food Rapid Detection, University of Shanghai for Science and Technology, Shanghai 200093, China*

Huajie Gu − *School of Chemistry and Life Sciences, Suzhou University of Science and Technology, Suzhou 215009, China*

Complete contact information is available at: https://pubs.acs.org/10.1021/acs.jafc.2c03626

Notes

The authors declare no competing financial interest.

■ ACKNOWLEDGMENTS

This work was partly supported by the Science and Technology Innovation Action Plan of Shanghai (20392001600) and the National Natural Science Foundation of China (32072312).

■ REFERENCES

(1) Malir, F.; Ostry, V.; Pfohl-Leszkowicz, A.; Malir, J.; Toman, J. Ochratoxin A: 50 Years of Research. *Toxins* **2016**, *8*, No. 191.

(2) Vidal, A.; Ouhibi, S.; Ghali, R.; Hedhili, A.; De Saeger, S.; De Boevre, M. The mycotoxin patulin: An updated short review on occurrence, toxicity and analytical challenges. *Food Chem. Toxicol.* **2019**, *129*, 249−256.

(3) Tao, Y.; Xie, S.; Xu, F.; Liu, A.; Wang, Y.; Chen, D.; Pan, Y.; Huang, L.; Peng, D.; Wang, X.; Yuan, Z. Ochratoxin A: Toxicity, oxidative stress and metabolism. *Food Chem. Toxicol.* **2018**, *112*, 320−331.

(4) International Agency for Research on Cancer. IARC monographs on the identification of carcinogenic hazards to humans. *Agents Classified by the IARC Monographs*, 2021, pp 1−130.

(5) Alshannaq, A.; Yu, J.-H. Occurrence, Toxicity, and Analysis of Major Mycotoxins in Food. *Int. J. Environ. Res. Public Health.* **2017**, *14*, No. 632.

(6) European Commission. Regulation Setting maximum levels for certain contaminants in foodstuffs *No. 1881/2006 of 19 December 2006 Off. J. Eur. Union.*, 2006; Vol. *364*, pp 5−24.

(7) Hajok, I.; Kowalska, A.; Piekut, A.; Cwielag-Drabek, M. A risk assessment of dietary exposure to ochratoxin A for the Polish population. *Food Chem.* **2019**, *284*, 264−269.

(8) Fan, Y.; Liu, F.; He, W.; Qin, Q.; Hu, D.; Wu, A.; Jiang, W.; Wang, C. Screening of multi-mycotoxins in fruits by ultra-performance liquid chromatography coupled to ion mobility quadrupole time-of-flight mass spectrometry. *Food Chem.* **2022**, *368*, No. 130858.

(9) Gao, X.-Y.; Xu, C.; Zhang, X.; Li, M.; Gong, X.; Yang, H.; Tang, J. Development of Fc-specific multi-biotinylated antibodies via photoreactive tandem AviTag repeats for the ultrasensitive determination of ochratoxin A. *Food Control.* **2022**, *132*, No. 108525.
(10) Zhang, S.; Luan, Y.; Xiong, M.; Zhang, J.; Lake, R.; Lu, Y. DNAzyme Amplified Aptasensing Platform for Ochratoxin A Detection Using a Personal Glucose Meter. *ACS Appl. Mater. Interfaces.* **2021**, *13*, 9472−9481.
(11) Hao, L.; Liu, X.; Xu, S.; An, F.; Gu, H.; Xu, F. A novel aptasensor based on DNA hydrogel for sensitive visual detection of ochratoxin A. *Microchim. Acta* **2021**, *188*, No. 395.
(12) Li, Y.; Zhang, N.; Wang, H.; Zhao, Q. Fluorescence Anisotropy-Based Signal-Off and Signal-On Aptamer Assays Using Lissamine Rhodamine B as a Label for Ochratoxin A. *J. Agric. Food. Chem.* **2020**, *68*, 4277−4283.
(13) Armstrong-Price, D. E.; Deore, P. S.; Manderville, R. A. Intrinsic "Turn-On" Aptasensor Detection of Ochratoxin A Using Energy-Transfer Fluorescence. *J. Agric. Food. Chem.* **2020**, *68*, 2249−2255.
(14) Lv, L.; Wang, X. Recent Advances in Ochratoxin A Electrochemical Biosensors: Recognition Elements, Sensitization Technologies, and Their Applications. *J. Agric. Food. Chem.* **2020**, *68*, 4769−4787.
(15) Tang, Z.; Liu, X.; Su, B.; Chen, Q.; Cao, H.; Yun, Y.; Xu, Y.; Hammock, B. D. Ultrasensitive and rapid detection of ochratoxin A in agro-products by a nanobody-mediated FRET-based immunosensor. *J. Hazard. Mater.* **2020**, *387*, No. 121678.
(16) Li, C.-c.; Hu, J.; Luo, X.; Hu, J.; Zhang, C. Development of a Single Quantum Dot-Mediated FRET Nanosensor for Sensitive Detection of Single-Nucleotide Polymorphism in Cancer Cells. *Anal. Chem.* **2021**, *93*, 14568−14576.
(17) Yuan, N.; Zhang, Y.; Xu, H.; Zhou, Z.; Lu, X.; Chen, T.; Yang, Q.; Tan, J.; Zhang, W. Development of the Saltatory Rolling Circle Amplification Assay for Rapid and Visual Detection of Alicyclobacillus acidoterrestris in Apple Juice. *J. Agric. Food. Chem.* **2020**, *68*, 4538−4545.
(18) Li, Y.; Wang, L.; Zhao, L.; Li, M.; Wen, Y. An fluorescence resonance energy transfer sensing platform based on signal amplification strategy of hybridization chain reaction and triplex DNA for the detection of Chloramphenicol in milk. *Food Chem.* **2021**, *357*, No. 129769.
(19) Chai, S. Q.; Lv, W. Y.; He, J. H.; Li, Y. F.; Zou, H. Y.; Li, C. M.; Huang, C. Z. Highly Sensitive Detection of miR-21 through Target-Activated Catalytic Hairpin Assembly of X-Shaped DNA Nanostructures. *Anal. Chem.* **2021**, *93*, 14545−14551.
(20) Kim, K.; Jo, E.-J.; Lee, K.; Park, J.; Jung, G. Y.; Shin, Y.-B.; Lee, L. P.; Kim, M.-G. Gold nanocap-supported upconversion nanoparticles for fabrication of a solid-phase aptasensor to detect ochratoxin A. *Biosens. Bioelectron.* **2020**, *150*, No. 111885.
(21) Liu, R.; Ali, S.; Haruna, S. A.; Ouyang, Q.; Li, H.; Chen, Q. Development of a fluorescence sensing platform for specific and sensitive detection of pathogenic bacteria in food samples. *Food Control.* **2022**, *131*, No. 108419.
(22) Liang, Z.; Hao, C.; Chen, C.; Ma, W.; Sun, M.; Xu, L.; Xu, C.; Kuang, H. Ratiometric FRET Encoded Hierarchical ZrMOF @ Au Cluster for Ultrasensitive Quantifying MicroRNA In Vivo. *Adv. Mater.* **2021**, No. 2107449.
(23) Wang, G.; Yu, H.; Yang, L.; He, Z.; Zhou, L.; Sun, J.; Gu, X.; Yang, W.; Tang, B. Z. Core-Shell Fluorescent Polymeric Particles with Tunable White Light Emission Based on Aggregation Microenvironment Manipulation. *Angew. Chem., Int. Ed.* **2021**, *60*, 25246−25251.
(24) Roth, S.; Trinh, P. T.; Wachtveitl, J. Two-photon absorption enhancement for organic acceptor molecules with QD antennas. *Nanoscale.* **2021**, *13*, 9808−9815.
(25) Qiu, W.; Gao, F.; Yano, N.; Kataoka, Y.; Handa, M.; Yang, W.; Tanaka, H.; Wang, Q. Specific Coordination between Zr-MOF and Phosphate-Terminated DNA Coupled with Strand Displacement for the Construction of Reusable and Ultrasensitive Aptasensor. *Anal. Chem.* **2020**, *92*, 11332−11340.
(26) Walter, J.-G.; Koekpinar, O.; Friehs, K.; Stahl, F.; Scheper, T. Systematic investigation of optimal aptamer immobilization for protein-microarray applications. *Anal. Chem.* **2008**, *80*, 7372−7378.
(27) Lu, N.; Pei, H.; Ge, Z.; Simmons, C. R.; Yan, H.; Fan, C. Charge Transport within a Three-Dimensional DNA Nanostructure Framework. *J. Am. Chem. Soc.* **2012**, *134*, 13148−13151.
(28) Ge, Z.; Lin, M.; Wang, P.; Pei, H.; Yan, J.; Shi, J.; Huang, Q.; He, D.; Fan, C.; Zuo, X. Hybridization Chain Reaction Amplification of MicroRNA Detection with a Tetrahedral DNA Nanostructure-Based Electrochemical Biosensor. *Anal. Chem.* **2014**, *86*, 2124−2130.
(29) Zhang, J.; Wang, Y.; Zhao, X.; Chen, M.; Peng, Y.; Bai, J.; Li, S.; Han, D.; Ren, S.; Qin, K.; et al. Dual Sensitization Smartphone Colorimetric Strategy Based on RCA Coils Gathering Au Tetrahedra and Its Application in the Detection of CK-MB. *Anal. Chem.* **2021**, *93*, 16922−16931.
(30) Guo, H. Y.; Ruan, F. X.; Lu, L. H.; Hu, J. W.; Pan, J. A.; Yang, Z. L.; Ren, B. Correlating the Shape, Surface Plasmon Resonance, and Surface-Enhanced Raman Scattering of Gold Nanorods. *J. Phys. Chem. C* **2009**, *113*, 10459−10464.

https://doi.org/10.1021/acs.jafc.2c03626
J. Agric. Food Chem. 2022, 70, 10662−10668